



**SCHLUMBERGER VERTICAL SOUNDING
TECHNIQUES AND INTERPRETATIONS:
KRÍSUVÍK, ICELAND AND MENENGAI, KENYA**

Augustine W. Kanyanjua

**Geothermal Training Programme
Reykjavík, Iceland
Report 12, 1987**

ABSTRACT

The paper explores the application of the Schlumberger array and the consequent interpretation of the data the author participated in acquiring during the main project work session of the training program. Data from Krisuvík geothermal field was interpreted using the computer facilities at NEA - the field had been studied before this survey. The results arrived at and a comparison with the previous surveys have been discussed.

Data interpretation was done using modern programs particularly the LIKAN and the TULKUN which accommodate very minor features of the area under investigation and automatically computes and compares the modelled parameters to those of the field measurements. This include data from Menengai prospect area the author had participated in acquiring before attending the course in Iceland. The data is of high quality having a small weighed mean deviation of between 5% and 13%. However, owing to limited information at the time of interpretation only one dimensional interpretation was done on a selected profile nearest the Menengai crater. A low resistivity layer was detected at about two hundred meters depth, its resistivity tends to decrease towards the crater reaching a minimum of $10.6\Omega\text{m}$. Krafla field has been included as an example of how resistivity survey can lead to successful exploitation.

TABLE OF CONTENTS

ABSTRACT	iii
TABLE OF CONTENTS	v
LIST OF TABLES	viii
LIST OF FIGURES	ix
1. INTRODUCTION	1
2. DETERMINATION OF APPARENT RESISTIVITY	3
3. RELATIONSHIP BETWEEN RESISTIVITY AND HYDROLOGICAL FORMATION	4
3.1. General	4
3.2. Pressure	4
3.3. Temperature	5
3.4. Salinity	5
3.5. Effects of clays	5
4. DATA ACQUISITION	6
4.1. Introduction	6
4.2. Schlumberger configuration	6
4.3. Limitations	7
4.3.1. The current circuit	7
4.3.2. Potential circuit	8
4.4. Precautions	9
5. RESISTIVITY DATA INTERPRETATION	10
5.1. Introduction	10
5.2. Adjustment of curves	10
5.3. Model approximation	12
5.4. Iteration method	12
6. Modelling	15
6.1. One dimensional	15

6.2. Two dimensional	15
6.2.1. Introduction	15
6.2.2. The LIKAN program	15
6.2.3. The TULKUN program	16
7. KRÍSUVÍK HIGH TEMPERATURE FIELD	18
7.1. Introduction	18
7.2. Geological setting	18
7.3. Resistivity survey	19
7.4. One dimension modelling of the measurements .	20
7.5. Deductions from the model	21
7.6. Two dimension modelling of the measurements .	22
7.7. Results	23
7.8. Discussion	24
7.9. Conclusion	25
8. MENENGAÍ PROSPECT AREA	26
8.1. Introduction	26
8.2. Data interpretation	26
8.3. Results	26
8.4. Discussion	27
8.5. Conclusion	28
9. REVIEW ON KRAFLA HIGH TEMPERATURE FIELD	29
9.1. Introduction	29
9.2. Geological setting	29
9.3. Resistivity survey	30
9.4. Results	30
9.5. Discussion	30
9.6. Conclusion	31
ACKNOWLEDGEMENTS	32
REFERENCES	33
APPENDIX 1.	48
APPENDIX 2.	49

APPENDIX 3. 50

APPENDIX 4. 54

LIST OF TABLES

Table 1: Resistivity layers and corresponding
geohydrological formations in the Reykjanes
peninsula. 34

Table 2. One dimensional models of measurements in
Krisuvik high temperature area. 35

Table 3. One dimensional models of measurements in
Menengai prospect area. 36

LIST OF FIGURES

Figure 1. The Schlumberger array configuration. . . .	37
Figure 2. Schematic representation of ions absorbed in clay.	38
Figure 3. Dependence of electrical resistivity on temperature.	39
Figure 4. Shifts encountered during data acquisition of measurement TD101 in Krísuvík.	40
Figure 5a. Converging shifts in apparent resistivity.	41
Figure 5b. Nonconverging shifts in apparent resistivity.	41
Figure 6. Location of sounding line of measurement at Krísuvík.	42
Figure 7. Apparent resistivity at 600m depth in Krísuvík.	43
Figure 8. Location of measurements in Menengai prospect area.	44
Figure 9. Resistivity measurement lines at Krafla - Hvíthólar.	45
Figure 10a. Krafla - Hvíthólar; cross section of E - W resistivity distribution.	46
Figure 10b. Krafla - Hvíthólar; cross section of resistivity distribution perpendicular to the E - W direction.	47

1. INTRODUCTION

In the prospect phase of geothermal fields exploration, geophysical methods are an economical and powerful means of mapping the subsurface. The techniques adopted are dependent on the information desired. The Schlumberger array is best suited for improved vertical resolution to depths of up to about two km. For greater depth resolution magnetotelluric methods suit best.

Information sought in geothermal prospecting include faults, irregular shaped bodies, low resistivity bodies, caused by hydrothermal alterations, volcanic plugs, dikes etc.

Their characteristics are manifested in an equivalence form of resistivity readily detectable by the Schlumberger array. The configuration has been applied in the acquisition of all the data interpreted by the author, hence its description, operation, and limitation have been presented in detail.

Resistivity data interpretation comes in two categories - one dimensional and two dimensional. The one dimensional method assumes a horizontally layered earth of infinite lateral extent which fall short of the information necessary for a sound conceptual model. For improved resolution and a closer proximity to the substratum conditions, two dimensional models offer a clearer picture.

At N.E.A. the ELLIPSE, LIKAN and the TULKUN programs are used in the processing of data. The former is used in one dimensional interpretation while the latter two facilitate in the construing of a two dimensional model. However all the three programs come into operation at different stages since the final two dimensional model emanates from the simple one dimensional models obtained with the aid of the ELLIPSE program. These programs were used in the computation of resistivity data from Krisuvik field and Menengai prospect area in Kenya. A two dimensional model of a profile four km. long was construed from the measurements in Krisuvik. Due to lack of adequate information at the time of interpretation of the data from Menengai field only one dimensional interpretation was done.

Since Krafla field in north Iceland is a high temperature area and is utilized for electricity generation, the author found it relevant to Kenyan conditions. A review of the measurements and the subsequent interpretation is included.

2. DETERMINATION OF APPARENT RESISTIVITY

The apparent resistivity described all through this text is determined using the Schlumberger array shown in Figure 1. Section 4.2 describes the configuration in detail.

For a positive current I driven into the ground through a current electrode A and the current coming out of the ground through the electrode B. A potential difference δV is measured between two points M and N at the surface of the earth.

The voltage δV is given by;

$$\delta V = 2(PI/2\pi) \left[\frac{1}{(s-b)} - \frac{1}{(s+b)} \right] \dots \dots \dots (1)$$

Where, P is the apparent resistivity

I is the current

s is half the distance of the current electrode spacing

b is half the distance between the potential electrodes

The expression for apparent resistivity P_a is obtained by solving (1) for P , which yields

$$P_a = (\delta V/I) 24\pi s(s^2 - b^2)/4sb \dots \dots \dots (2)$$

The values of apparent resistivity P_a are plotted against s - usually designated as $AB/2$ - in a log - log graph paper. In the graph obtained, it is assumed that the earth is homogenous. The variations observed are a departure from this assumption. From the variations different models can be derived using different assumptions about resistivity distribution in the earth.

3. RELATIONSHIP BETWEEN RESISTIVITY AND HYDROLOGICAL FORMATION

3.1. General

The bulk of the earth's crust is predominantly of sedimentary nature. As to abundance, clays occupy the first places followed by sandstone, limestone and dolomites (M.P. Volarovich and E.I Parkhomenco. 1970). They are characterized by interstitial moisture content the amount of which is determined by the porosity ratio "k". Different values for a type of rock implies a variation in interstitial moisture contained within it.

Water saturated rock can be considered as a two phase system. The solid phase is represented by minerals such as calcite, quartz, etc. while the moisture content represents the fluid phase. The solid phase overwhelmingly possesses a very high resistivity in the order of $10^{10} \Omega\text{m}$. The fluid phase is an electrolyte of very high conductivity ($0.15 \Omega\text{m} - 10 \Omega\text{m}$). Because of the great difference in resistivity between the electrical resistivity of the fluid and solid phase, the main parameter that determine the electrical resistivity of the rock is the amount of the fluid contained in the rock. Since the mode of conductivity in the formation is electrolytic, the nature of the electrolyte becomes of paramount importance in understanding the resistivity exhibited. Temperature, pressure and salinity all have an effect on the nature of the fluids resistivity.

3.2. Pressure

Experimental and theoretical work show that, the resistivity of water saturated rocks increase with hydrostatic pressure and decrease with an increase of pressure in the formation (Dobrymin, 1970 & Avchyan, 1971) The extent of the increase of pressure within the formation is a function of porosity, rock structure, type and cement content.

3.3. Temperature

Figure 3 shows variation of resistivity with temperature in a variety of rocks. Greatest changes occur between 20°C and 150°C. Resistivity decrease with temperature in a water bearing rock up to about 300°C beyond which a sharp increase is observed. The temperature increase lowers the viscosity of water resulting in high mobility of the ions present.

3.4. Salinity

It plays the most important role in electrolytic conduction. Current conduction results from the dissociation of the dissolved salts into ions. Since each ion can carry only a definite quantity of charge, it follows that the more ions available in solution the faster they will travel and the greater will be the charge that can be carried.

3.5. Effects of clays

Resistivity in clays is particularly important as it features prominently in the upper strata. A very high value in porosity constant "k" - between 20% and 50% - is observed. The solid phase too contributes a great part in conduction. Acting as an additional path to the electrolytic conduction. The resistance of this path is usually low. Abnormally high conductivity is encountered in the double layers (fig.2) between the pores and the minerals. The cations are required to balance substitution and broken bonds (H. Ward and W. Sill, 1983). High conductivity in all rocks containing clay minerals can be attributed to this factor. In a geothermal environment, hydrothermal alteration converts feldspar to kaolinite, montmorillonite and other clay minerals. In basic rocks, chlorite and serpentine can also be produced (H. Ward and W. Sill). All these alterations produce high surface conductivity.

4. DATA ACQUISITION

4.1. Introduction

The aim of resistivity measurements is to obtain the electrical properties of the earth's bedrock which can be viewed as a reflection of the strata's formation at different depths. Various techniques are employed depending on the information needed. In geothermal prospecting, dipole - dipole and Schlumberger configurations are mostly preferred. The dipole - dipole array is well suited to combine sounding and profiling in which application it provides modest vertical and lateral information. For improved vertical resolution the schlumberger array is most convenient. Current that penetrates the strata creates a potential difference between the potential arms of the array. The magnitude of penetration is related to the current - arm length. Thus, electrode separation, current injected to the ground and potential caused by this current are used to delineate resistivity at various depths.

4.2. Schlumberger configuration

Four electrodes are symmetrically positioned along a straight line with the current electrode on the outside and the potential electrodes at the inner part of the array (fig. 1) Under working conditions the current electrode separation is referred to as AB while that of the potential electrode separation as MN. The depth to which the current penetrates is varied by altering the length of AB. The extent to which the subsurface can be depicted is proportional to AB spacing. When the ratio of AB to that of MN becomes too large, the potential electrodes must be displaced outward or else the potential difference received becomes too small to be measured with reasonable accuracy. At the beginning of a series of measurement, the distance MN must be greater or equal to $AB/3$.

However, experience has shown that when MN is greater or

equal to $AB/5$ reasonable accuracy is attained for short AB spacing.

When the current electrodes are displaced it is necessary to carry out measurements at all the positions of the potential electrodes for the same current value. Unless the signal is too small to be detected which occurs with the innermost potential electrodes. Preferably, repeat measurements should be carried out at several consecutive values of the current electrode spacing. This procedure provides some information on the effect of potential electrode displacement upon measurement.

4.3. Limitations

4.3.1. The current circuit

The current used in resistivity sounding is direct current but for practical reasons discussed in the potential circuit it is necessary to carry out repeat measurements with alternating directions of the current flow through the ground. The reversion in direction implies that the current is not DC in the strict sense. As a result there is a tendency of the current to concentrate toward the near surface of the earth. The phenomenon is known as the "skin effect." It introduces the inherent characteristic of an alternating current propagation. Under conditions whereby a direct current field would be homogenous the current density of an alternating current would decrease exponentially with depth. Penetration would be dependent on frequency and the resistivity of the ground material. However, for very low frequencies the deviation from the conditions of a strict DC medium is negligible. Under operating conditions the skin effect manifests itself in a manner that when the current is switched on it requires sometime to build up to its final value; and when the current circuit is switched off voltage difference takes sometime to fall to zero. Time allowance should therefore be given for current to build up to its optimum value and to fall to zero on opening the circuit.

4.3.2. Potential circuit

During the measurements of the potential difference between two points on the ground, polarization potentials are generated at the contact between an electrolytic conductor and a metallic conductor. The magnitude of these potentials is affected both by composition of the metallic conductor and that of electrolytic solution. The electrolytic conductor in this case is the ground water whose composition cannot be kept under control. This difficulty can be overcome to a high degree by using "porous pot" electrodes. They consist of a ceramic vessel filled with a copper sulphate solution kept in contact with a copper wire.

Whenever a potential difference is being measured, the potential itself changes the quantity being measured. The reason being that the potential measuring acts as a parallel circuit which diverts current from its flow through the ground leading to an underestimate of the measurement taken. This effect cannot be entirely eliminated but its magnitude can well be kept within acceptable limits. In a parallel circuit the electric current divides over the branches so that the current intensities in the separate branches are in inverse proportion to the resistance of the branches. Thus, if the resistance of the potential measuring device is sufficiently high, then only a small fraction of the current through the ground will be diverted into the measuring circuit and the change in current density in the ground will be negligible. This entails the use of voltmeters with sufficiently high internal resistance.

Electrical currents always flow in the ground even when there is no current injected at the electrodes this are partly due to natural causes and partly caused by electrical leakages from industrial installations. Collectively they are referred to as "parasitic currents." The measured current is partly due to the existence of these currents. It is therefore extremely important to eliminate them as far as possible. This cannot be completely done because their magnitude and direction are not always constant.

Consequently their variation remain a source of error through out the measurement.

4.4. Precautions

As observed in the discussion above a lot of inhibitions against perfect measurements exist. However, certain precautions adhered to give way to very high quality data. The effect of parasitic current can be reduced appreciably by selecting a site far from underground pipes, transmission cables, underground pipes, and wire fences particularly if they are earthed or electrified. Rail roads, asphalt roads and overhead cables should also be avoided.

Electrode cables should be well insulated or else current leakage would lead to erroneous determination of magnitude and the point of current injection.

The solution in the porous pots should remain saturated.

This can be verified by ensuring crystals always occur in the solution.

Loose earth surface normally results in poor contact of the current electrodes with the ground. Connecting two or more electrodes in parallel increases the surface area of the electrode in contact with the ground resulting in an improved measurement. Owing to the high voltage used in the current arms good communication between the center and the terminals is necessary. As an additional precaution all connections handled by hand should be insulated.

5. RESISTIVITY DATA INTERPRETATION

5.1. Introduction

The objective of resistivity data interpretation is to delineate the resistivity values obtained with actual conditions in the earth's formation. Assumptions which do not occur in real practice are often made. Approximate models can be derived from the graph obtained in equation (2). Further refinement and closer approximation can be achieved by the iteration technique and two dimensional interpretation methods all of which are discussed below.

5.2. Adjustment of curves

As mentioned earlier it becomes necessary to increase the potential electrode spacing as the distance between the current electrodes is increased, without which the potential difference between the electrodes would become too small to allow reliable measurements. Changing the potential electrodes entails taking the potential at two or more points of the current electrodes. The apparent resistivity graph thus obtained show segments represented by these points which in most practical cases fail to tie with other parts of the graph within an acceptable error limit. Figure 4 is a typical example obtained by the author during a resistivity survey in Krisuvik high temperature field. The shifts in this case are small and have been adjusted by the automatic inversion technique in the computer program ELLIPSE available at NEA. The reason for this can be partly attributed to "eccentricity" - the ratio of the current electrode spacing to that of the potential arms. A big contrast in apparent resistivity of two consecutive layers often results in a tie-in failure in both cases the types of shifts encountered are of the convergence type as shown in figure 5a.

Occurrence of inhomogeneities in the near surface of the earth's strata results in the distortion of the current pattern and a relative change in current density. The extent

to which this takes place depends on the position of the measuring points with respect to the inhomogeneities. This arises to non convergent shifts illustrated in figure 5a. Convergent and non convergent shifts are corrected by filter coefficients of the inversion technique. At NEA the ELLIPSE program automatically makes this corrections. Curve slopes should be carefully checked as there exists a theoretical limit to the angle of inclination on the ascending part of the curve. The ascending part can take any value. Ascents are encountered when a very high resistivity contrast exists at two adjacent layers. Taking an example of two consecutive layers where the upper layer has a finite resistivity, say ρ_1 and the underlying layer has an apparent resistivity ρ_2 where ρ_2 is far, far greater than ρ_1 . A current injected from the surface will cause a potential drop δV which will depend on the value ρ_1 .

Theoretically ρ_1 can any value from zero to infinity meaning the descending slope can take any value from zero to ninety degrees. When the electrode spacing is comparable to the overburden thickness much of the current will flow along the boundary and the voltage drop reading will be constant. Taking the electrode spacing as s . When s exceeds the boundary thickness we have;

$$\rho_1 = \rho_2$$

where t is the thickness of the first layer.

Since the resistivity of the lower layer ρ_2 is very high compared to ρ_1 , the lower layer acts as an insulator and the current density will be infinitely higher in the upper layer.

Taking two points x and y on the ascending part of the graph, the following relationship holds.

$$\rho_x = S_x \rho_1/t \dots\dots\dots(1)$$

$$\rho_y = S_y \rho_1/t \dots\dots\dots(2)$$

Combining (1) and (2)

$$\rho_Y/\rho_X = S_Y/S_X$$

for which

$$(\log \rho_Y - \log \rho_X) / (\log S_X - \log S_X) = 1$$

which is a slope of 45 degrees.

Obtaining a bigger value on the ascending part of the curve would indicate an erroneous measurement or a possible inhomogeneity near the surface.

5.3. Model approximation

In this case the model referred to is the resistivity of different layers of the bed rock and their corresponding depth at the center of the measurement. The data collected in the field is used to make a one - dimensional model which normally proves a good starting point for more refined models.

As a starting point in the inversion, it can be taken as a rule that a resistivity curve takes a new turn when traversing a new layer. The depth at which this takes place can be assumed to be roughly equal to half the distance of the electrode spacing at that point. This depth and the corresponding resistivity value are taken as the approximate model. Difference in depth of two consecutive layers is taken to be the approximate thickness of the lower layer.

5.4. Iteration method

A point source on the surface of a horizontally layered earth gives way to potential at the subsurface V_i where i refers to the several layers of the substratum. For the potential at the surface the equation is;

$$V = I_2 \rho_1 \pi \int [1+2\theta(\Gamma)] J_0(\Gamma_r) d\Gamma$$

Where ρ_1 -- resistivity of the first layer
 I -- the current
 r -- the distance of the current source from the
measuring point.
 Γ_r -- A variable of integration.

The function $[1 + 2\theta J_0(\Gamma_r)]$ is the Slichter kernel function and can be used in its relationship with the Perkins recurrence solution to work out the resistivity of the subsurface strata σ_i .

The resistivity of any layer according to the Perkins recurrence solution is given by the expression

$$K_i = [K_{i+1} + \rho_i \tanh(t_i \Gamma)] / [\rho_i + K_{i+1} \tanh(t_i \Gamma)]$$

where K_i is the Slichter Kernel function of the shallowest layer that occurs in the sequence under consideration.

Koefoed (1970) introduced the resistivity transform function.

It is defined by the equation

$$T_i = \rho_i * K_i$$

Where, T_i is the transform function
 ρ_i is the resistivity of the layer
 K_i is the Slichter kernel function

expressed in the resistivity transform, Perkins recurrence relation is

$$T_i = [T_{i+1} + \rho_i \tanh(t_i \Gamma)] / [1 + T_{i+1} \tanh(t_i \Gamma) / \rho_i]$$

In the reverse sense the equation is given by the following expression;

$$T_{i+1} = \frac{[T_i - \rho_i \tanh(t_i \Gamma)]}{[T_i \tanh(t_i \Gamma / \rho_i)]}$$

Transform functions are easier to work with because of their close physical relation with apparent resistivity as a function of electrode spacing. This can be improved by the use digital linear filters. Samples of one function are taken at a constant interval along the abscissa and expressed linearly in the sample values of the other function. The coefficient so applied are known as filter coefficients. The accuracy achieved depend on the number of filter coefficients adopted.

The ELLIPSE program enables the comparison in sample values derived from apparent resistivity transform of the data obtained in the field measurement and resistivity transform models computed from the model parameters. The least square method is used to weigh the deviation. Table 2 & table 3 show the results of the application of this method by the author during the iteration interpretation of Kísuvík high temperature field and Menengai prospect area in Kenya.

6. Modelling

6.1. One dimensional

An approximate model used as the starting point in the iteration program yields a refined model of the strata at the approximate location of the sounding center. Iso - resistivities are plotted to give a one dimensional conceptual model. Ranges are selected from the observation made.

Appendix 1 shows a one dimensional model the author arrived at after interpretation of data from Krisuvík high temperature field.

6.2. Two dimensional

6.2.1. Introduction

A two dimension model closely approximates to the actual substratum conditions observed in the earth. Vertical contacts anomalies like dipping beds and conductive overburden are all assumed absent in a horizontally layered earth considered in a one dimension model. (Mwangi; 1982) The program LIKAN and TULKUN available at NEA enables the achievement of a very high degree of accuracy owing to the large number of elements used.

6.2.2. The LIKAN program

This program facilitates the construction of a two dimension model drawn from the one dimension model described above. By careful observation of the trend in resistivity distribution and their corresponding thickness at consecutive centers, vertical boundaries are introduced.

Taking an example of a layer say at twenty meters depth and with an apparent resistivity ρ_a . It might be observed that a similar layer at a comparable depth exists from the adjacent center of measurement but with a slightly higher or lower

apparent resistivity value. A vertical boundary can be introduced at a point midway between the two centers. Locating the most appropriate position comes with experience. Boundaries of this kind are introduced on the entire length of the sounding profile.

For higher accuracy, vertical boundaries within the area of measurement are more closely spaced. The neighboring zones of the area under measurement are simulated by assuming conditions of their immediate neighborhood with the model. The layers in the model are assumed horizontal but the thickness can be varied at different sections depending on the one dimensional observation made.

A model obtained in this manner is represented in the form of a grid consisting of blocks defined by their lateral and vertical position as well as apparent resistivity values. The blocks are referred to as elements and their vertices as nodes. The position of each node is described by Cartesian coordinates (x,z) . Appendix III. illustrates models made by the author from Krísuvík field data in the program LIKAN. The grid is further subdivided into finer segments which take a triangular shape. The "mesh" or triangular net obtained is stored in an output file for further processing in the TULKUN program.

6.2.3. The TULKUN program

Appendix II shows the triangular net of a model from the LIKAN Program. In the TULKUN program, by virtue of the resistivity and position of each triangle the potential at the edges are calculated (Zhou, Zhen, and Eyjólfsson) by the finite element method (FEM). It is considered that owing to the extremely short distances between the edges of the triangles the change in potential from one point to the next is linear.

The program computes the apparent resistivity values and electrode spacing of the model. The accuracy of the model relative to the actual conditions in the substratum is derived by comparing the computed plots from the model with

those obtained from the field data. This is known as fitting. For an ideal fit all points on the measured resistivity graph should tally with those computed from the model.

7. KRÍSUVÍK HIGH TEMPERATURE FIELD

7.1. Introduction

Krísuvík high temperature field covers an area of approximately 40 km² in the central area of the Reykjanes peninsula. It is overlain by two ridges separated by a valley in between. The area is manifested with steam vents, hot springs and highly altered bedrock due to acid surface leaching. Geological, geochemical, and geophysical surveys have been carried out since 1970. Several exploratory wells ranging from 800 to 1000 meters deep have been drilled. The bedrock is characteristic of the Reykjanes peninsula, dominated by very highly permeable lavas that result in the penetration of sea water into the relatively shallow water table of the area. This is however not reflected in the local topography. Resistivity and magnetotelluric measurements indicate a highly resistive upper layer. The resistivity decreases with depth from about 200 meters below the surface to a very low value of less than 3 Ω m at about six hundred meters. A sharp rise is observed at layers below 2.5 km depth. This is in close agreement with temperature measurements carried out in the drilled wells. Section 7.3 to 7.9 of this report reveals the findings of a resistivity survey the author undertook as an extension study of the area. A Schumberger configuration was used at six centers along a profile 4 kilometers long running across the valley and the two ridges in the 100 deg.(N.W) direction.

7.2. Geological setting

The field is located in the Reykjanes peninsula, a sub aerial continuation of the crest of the mid - Atlantic ridge into Iceland. It is characterized by steep sided mountains of pillow lavas and hyaloclastites which protrude through the lava fields. All rocks are of basaltic composition. Numerous activities have occurred in recent history - the latest was 1100 years ago - within the vicinity of the field.

The activity consists of fissure eruptions as well as central magma eruptions the latter being more voluminous. Prolonged activity tends to have been concentrated in a single vent although the magma may initially have protruded through a fissure resulting in volume edifices on one hand and fissure edifices on the other.

The area under investigation lies on a plate boundary where a fault swarm crosses the boundary at an angle of 30 to 40 degrees (Klein, Einarsson, and Wyes, 1973). Topographically the area is characterized by two major southwest striking hyaloclastite ridges. Between them lies a valley covered with lava flows. All surface manifestations are found within these ridges. From the information gathered on the formation of the ridges, it is apparent that volcanic activity has been more intense on the ridges than on the valley. Further revelation infer that the fissure swarm that dissects the area is more dense within the ridges than in the lava covered valleys. It is also true that tectonic activity has been more intense on the ridges where volcanic activity was most intense. (Arnórsson, Björnsson, Gíslason; 1975)

The bedrock of the area is composed of very permeable rock especially the lava flows. This is strongly reflected in the salinity of the underground water system which is comparatively higher to that of similar fields outside the Reykjanes peninsula. Observations from test wells drilled in the area indicate an inverse thermal gradient between 400 and 600 depth. No conclusive flow model has yet been perceived.

7.3. Resistivity survey

A Schulumberger configuration was used on the six preselected centers. Prior to this survey, more than 150 DC soundings with the Schlumberger array had been made. Dipole-dipole, and magnetotelluric measurements aimed at mapping the subsurface have been made too.

The general pattern of resistivity distribution at comparable depth show close agreement with previously done measurements. High resistivity is predominant at the surface except in

areas where there has been strong alteration due to acid surface leaching. Resistivity drops rapidly from about a depth of 200 meters reaching a minimum of under 5 ohm meters at about 500 meters below the surface in some areas. The measurements were expanded to a maximum electrode spacing of 1780 meters at each of the six centers designated TD98, TD99, TD100, TD101, TD102 and TD103. They were so chosen that the current arms of the array overlapped with those of the neighboring centers. This is particularly helpful in identifying and locating strong lateral resistivity variation which could otherwise be attributed to erroneous measurements. Since the area is topographically very inhomogeneous with the highest point being well over one hundred meters in altitude over the lowest, a cross - section of the profile was made by taking the altitude at every 50 meters over the entire length of the profile.

7.4. One dimension modelling of the measurements

An approximate model of each of the centers is made as described in section 6.1 of this report. Figure 6 shows the location of the sounding centers, a better display of their location is shown on the cross - section of the profile (Appendix III). The ELLIPSE program is used to refine the one dimensional models from the approximations previously done. Twenty to thirty iterations were made for each sounding the number of inversion chosen depending on the number of layers accrued from the particular model. All models indicate a modest deviation between 5% and 13% with the exception of TD101, which has a 22% deviation it is also characterized by converging shifts described in section 5.2

It is also noteworthy that resistivity at the surface is 300 Ωm decreasing to 3 Ωm at about 100 meters depth. Thus, big resistivity contrast is evident which explains the exceptional nature of the curve. Poor electrode contact with the ground was also experienced on one of the current arms.

7.5. Deductions from the model

The 1-D model conceived portray a strong resemblance with those from previous measurements - high resistivity that rapidly decreases with depth. The rate of drop being mostly determined by the location of the measurement. TD98 and TD100 are located on the flat basin between the ridges show a small mean deviation of 5.2 % and 4.18 % respectively. The sequence of layer thickness and resistivity are similar. However, a marked difference arises at depth below 200 meters. Continuity of low resistivity prevails at the center TD98 while at TD100 which is nearer the hills a thin layer about 20 Ωm appears this is due to a thin extension of a higher resistivity layer observed at the same elevation on the measurement done on the adjacent sounding center. The uppermost layer of the basin is characterized by very high resistivity which might indicate unaltered formation. It extends to the slopes and the top of the ridges of the profile except at TD99 and part of the area taken at the measurement center TD102 which borders it. The area is in a section of the field that is characteristic of steam vents. Resistivity is in the order of 50 Ωm which is comparatively lower than that of the surrounding regions which go to values of several hundred Ωm . The influence of this layer is detected at TD98 which has a slightly lower resistivity value at the surface than TD100. Very low apparent resistivities ranging between

2 Ωm to 4 Ωm are predominant below the two ridges. The bottom most layers of TD101 and TD102 both of which are on the hills indicate this. The phenomenon is observed in the third layer at a depth of between 200 and 150 meters under the north eastern part of the profile.

This could indicate an upflow zone. The upflow encounters a highly permeable bedrock about 900 meters to the north of TD98. There is a lateral expanse of low permeability in this direction paving way to the presence of brine hence low resistivity. The permeability or presence of brine increase with altitude. Below TD101 and TD100 but wanes under the

next sounding center TD98. This could be due to a vertical boundary the presence of which might be detected by two dimensional interpretation. At a similar altitude the same pattern is characteristic in the southern ridge the distinction being that the resistivity encountered in this case is of the order of 20 Ω m to 50 Ω m lying under the highly resistive surface layer.

On close scrutiny of the model it was observed that additional sounding at about 500 meters from each of the measurement centers at the edge of the profile - TD103 and TD101 - would be necessary. They would be particularly helpful in identifying the parameters of the high resistivity layers observed at about 250 m and 150 m below the surface of the N.E and S.W ridges respectively.

7.6. Two dimension modelling of the measurements

The two dimension model of the field was done with the aid of the LIKAN and TULKUN programs described in section 6.2 and 6.3 of this report. The aim is to locate more exact positions of the boundaries encountered in resistivity distribution - both vertically and laterally. The TULKUN program has the extra advantage of accommodating very minor changes within the model including the topography. It also fits the model automatically rendering a very high degree of accuracy at the very end.

The model was simulated on both sides of the profile - to enhance accuracy - assuming the conditions of the extreme ends of the measured part of the field. Apparent resistivity thickness and altitude was assumed uniform over the simulated segments that stretched a distance of eight thousand meters on both sides of the profile.

Unlike in one dimensional interpretation, though horizontal layers are included the thickness of a particular section of a layer can be altered by changing the parameters of the element, thus eliminating uniformity in thickness within a layer. An element can be split into a pair of triangles with different resistivities adding further resolution to the

model. In practice these could represent anomalies like fissures, thin dikes, vertical boundaries dipping contacts and round bodies. In the final model a phenomenon of this kind is particularly common under the sounding TD99.

The splitting of elements were added to position parts of the intermediate layers without affecting the neighboring measurements.

In all, a total of 234 elements were used in the model. To refine it into "finite elements" the elements were subdivided into 3673 triangles out of a possible 5000 the program is capable of allocating to a refined triangular net.

7.7. Results

A low resistivity layer about 100 meters thick exists right beneath TD99 from the one dimension model observation. The pattern of this low resistivity becomes more complex indicating a tendency of low resistivity towards the surface layer of the peak between TD99 and TD102, which interestingly is the only section of the measured area that shows signs of low resistivity near the surface. Appendix I shows the anomalous high resistivity zone (about 25 Ωm) at a depth of 100 meters was found to be further to the north east and deeper by about 50 meters. The highly resistive bed at the extreme end of the south western part of the profile is narrower than indicated in the one dimensional model.

Intermediate layers - between 50 and 100 meters - beneath the valley were found to contain anomalies of high resistivity above 100 Ωm . A sharp contrast with the surrounding whose resistivity is of the order of 20 Ωm to 50 Ωm . This had passed undetected in the one dimension model.

The final model was arrived at after twenty fittings. All the computed measurements showed a close agreement with the measured ones. Appendix III shows a series of the models fitted at different stages before the final one was construed. A marked similarity with the one dimension model is observed. The few discrepancies prevalent are stated.

7.8. Discussion

It has to be noted that the measurement taken were too few to depict a very clear picture of the entire field which covers an area of about 40 square kilometers compared to the 4 kilometers investigated in this survey. Hence, the results obtained cannot be accrued for the entire field nevertheless it should be observed that there is a close agreement with previous surveys.

Conventionally, fluid conduction explains low resistivity within the earths formation. The nature of the fluid plays a major role in estimating the dominant mode of conduction. Salinity and temperature being of paramount importance. The brine give rise to higher electrolytic conduction while the temperature lowers the viscosity of the fluid enhancing the mobility of the ions present - this holds only up to 300°C (Ward & Sill 1983) Table 1 shows resistivity for different hydrogeological formations of the bedrock in the Reykjanes peninsula. Low resistivities observed at Krísuvík fall within the ranges of brine of geothermal and sea water origin. Presence of fresh water in the bedrock is evident owing to the high permeability of the predominant lavas and the high level rainfall (800 mm/year) and lack of surface run off (Georgsson L. 1984).

Given the inherent equivalence characteristic of resistivity data interpretation, limited concrete conclusions can be made directly. The observation on resistivity pattern can be related to the hydrothermal studies that have been made on the field of which the most important are from the exploratory wells. The principal aim behind drilling was to reveal underground temperatures in different parts of the hydrothermal area and "calibrate" the results of the resistivity survey. Temperatures rather than salinity and porosity were deduced as the major factors causing presence of the low resistivity observed at depth. To what extent each is responsible is still uncertain. Maximum temperatures are observed at about 450 meters as in well H5. This coincides with the low resistivity zone (fig. 7) below 450

meters an inverse temperature gradient is imminent.

7.9. Conclusion

All the drilled wells show an inverse thermal gradient below 450 meter depth. Despite strategy in their location, similar characteristics are persistent disproving the "cone sheet model" that implies a single heat source.

Though not enough measurements were taken over the ridges to depict clearly the resistivity distribution beneath them, the best fitting two dimensional model indicate the presence of two low resistivity zones right under the ridges separated by a high resistivity barrier. This could indicate the presence of two different upflow zones. The source of the geothermal brine involved seem to be the region under the ridges where tectonic activity has been most intense.

8. MENENGAI PROSPECT AREA

8.1. Introduction

About 100 Schlumberger soundings were carried out in the area between November 1986 and April 1987. This part of the report discusses the one dimensional results obtained from the data of the profile marked AB on figure 8 lying nearest the crater in the NW - SE direction.

The selected profile consists of six sounding centers designated at the time of interpretation as TD1, TD7, TD9, TD15, TD16 and TD17 stretched over a distance of thirty kilometers. The maximum electrode spacing varies between 3000 and 4000 meters on each arm of the array. The data was interpreted with the aid of the ELLIPSE program described in section 5.4 of this report.

8.2. Data interpretation

Variation of the electrode spacing with resistivity is determined by feeding the field data in the ELLIPSE program. The graphs obtained were used to estimate the approximate parameters of the layers and their corresponding apparent resistivity values for use at the initial stage of the iteration method described in section 6.4.

8.3. Results

The curves obtained from the field showed great similarity - all comprise of three layers except TD7 which has four. The bottommost layer has the lowest resistivity while the medium layer indicate the highest resistivity value with the exception of one - TD7. Twenty inversions were made for each model. The number of inversions enhances the accuracy of any model obtained in the ELLIPSE program. In the case of these measurements little or no improvement could be achieved with more than twenty iterations.

The weighed mean deviation was reasonable. The highest value

obtained was 16.8% in the measurement TD1, the rest had a modest values ranging between 13.54% and 5.56%. Table 3 show the details of every model of the six measurements under consideration.

8.4. Discussion

The resolution of the model is of low degree being uni - dimensional. Not enough information was available to construct a two dimensional model.

It is observed that the surface layer is between 2 and 10 meters in thickness with an average resistivity of about 50 Ω m. This holds for the entire profile with TD7 being the only exception. This can be attributed to the clays on the surface whose range of resistivity agree with that observed. The intermediate layer has a consistently high resistivity value varying slightly from one locality to the other. Ranges are in the order of 150 Ω m. A correlation in depth and resistivity is somewhat apparent though not to a significant extent. Decreasing values are observed where the layer tend to thicken towards the subsurface.

Apart from TD17 the other five measurements indicate a bottom layer at a depth between 115m and 230 meters. The layer shows uniformity in depth at 200 - 235 meters under four of the configuration centers - TD15, TD16, TD7 and TD16.

Particular attention should be paid to this layer since fairly low resistivities are observed. The lowest in this case being 10.6 Ω m measured at the center TD7. The other measurements show a value between 16 Ω m and 25 Ω m at roughly the same depth. On careful observation of the resistivity distribution within the layer, it becomes obvious there is an East - West trend in resistivity variation. Measurements nearest the crater have the lowest resistivity which increases proportionally with distance between the center of measurement and the crater. Resistivity variation pattern of the bottommost layer with the distance from the crater is of particular interest. Considering the resistivity values in this zone do not vary greatly with those of productive fields

of similar geological formation, it is possible that geothermal potential exists. More measurements closely spaced to enable two dimensional modelling would yield interesting results.

8.5. Conclusion

Apart from being too few the measurements done were too widely spaced to draw conclusive results from. The existence of low resistivity at this stage can be related to the geochemical, hydrogeological, and geological studies to reveal to what extent it could be due to presence of faults and fissures, permeability, salinity and underground temperatures.

9. REVIEW ON KRAFLA HIGH TEMPERATURE FIELD

9.1. Introduction

In the summer of 1983, the NEA undertook a geophysical survey in the Hvíthólar area of the Krafla high temperature field. It was aimed at studying the size of the geothermal area by mapping low resistivity areas and follow fissures and faults within the region which might work out as aquifers. Schlumberger sounding and head - on profiling were done over an area of 1.6 square kilometers. A review of the findings is given below.

9.2. Geological setting

The geothermal field belongs to a volcanic active area - the most recent activity having occurred between 1975 and 1984. It is a central volcano north -east of Mývatn which is cut by a 100 km long NNA - SSW fissure swarm. In the center of the volcano lies a 100,000 years old caldera filled with sediments and lava. Most of the geothermal heat in Krafla is related to a magma chamber that lies at a depth of three to seven kilometers beneath the caldera. Recent activity has been confined within the fissure swarm nearest to the caldera. Repeated activity has occurred since 1975 in the fissure between Þríhyrningar and Dal fjallshryggur. Ring fractures are connected to the Krafla caldera with a an east - west lying trend by Hvíthólar. Fissures with a NE - NW bearing are related to some intrusive volcanism at the margin of the caldera. Steam flow has increased since reactivation started in 1975. Geothermal heat is closely connected to three main features; it occurs in the areas where the fissure swarm overlies the western most magma chamber at Leirhnjúrkurs, Víti, Hveragil, and Suðurhliðar found at the south of the caldera. (Fig.9)

9.3. Resistivity survey

Schlumberger soundings and head - on profiling were simultaneously used in the Hvíthólar area. By using both methods on the same line better information is gained on the resistivity of some geological sequence down to the depth of 800m to 400m than would have been achieved using either separately (Axel Björnsson. 1983).

The aim of the study was to locate low resistivity barriers as well as determine resistivity changes which might be related to variation in the country rock and the fracturing in the area. Measuring lines were put perpendicular to the main fissure swarm and the east - west fracture trend connected to the southern edge of the Krafla caldera. Special attention was paid to the landscape which is very rugged and measurements previously done for possible utilization in the interpretation. A total of 32 measurements were interpreted on four lines with a north - south trend and on one with an east - west trend.

9.4. Results

Measurements went on fine except for one which was disturbed by drill holes and pipes.

Interpretation of the data from the area has in general inferred two simplified models through the Hvíthólar area. Figure 10a and 10b show two sections of resistivity distribution in the subsurface on a N-S and E-W trend respectively.

9.5. Discussion

Good correlation is found between resistivity and geological sections made from drill holes. The resistivity high anomaly in the uppermost 250 to 350m in the drilling area is found to be in beds where glass basaltic layers are most apparent. Low resistivity layers from the depth of 250m down to 600m is found in tuff beds. Temperature profiles from drill holes by

Hvíthólar show the highest temperature at this depth interval whereas the best aquifers are found at the boundaries of the same low resistivity layer. Further connection between resistivity and geological sections are less certain. Beds to the east of Leirhóll have neither been studied nor is it known whether geothermal heat exists though resistivity measurements indicate an apparent low resistivity layer.

9.6. Conclusion

There is a relationship between geothermal and heat at Hvíthólar and the tectonic history of the area. It occurs at the surface where the N-S fracture cuts the E-W lying fracture zone at the edge of the caldera. Very low resistivity is only measured in a limited area around the hot springs at Hvíthólar. It alludes that the geothermal area is rather small and fixed to a limited channel outflow. Studies already done do not provide enough information as to whether the geothermal area at Hvíthólar could be only a limited spot of high heat.

ACKNOWLEDGEMENTS

I am grateful to the UNDP for awarding me the fellowship. The staff of U.N.U; Dr J.S. Guðmundsson for a well organized course, Dr B. Eyjólfsson my advisor for his active part in the training, Mr O.B Smárasson who took a lot of care on my welfare during my stay in Iceland.

I owe special gratitude to Gylfi Páll Hersir whose guidance in two-dimensional modelling was overwhelmingly helpful. And finally I would like to thank all the people of Iceland whose hospitality has made my stay seem so short lived.

REFERENCES

- Arnórsson, S. Björnsson, A. Gíslason, G. 1975: Systematic exploration of the Krísuvík High - temperature area, Reykjanes peninsula, Iceland. Proceeding Second UN Symposium on the development and use of Geothermal Resources. Vol 2 pp 853 - 863.
- Björnsson A. 1984: Geophysical reconnaissance of Krafla-Hvithólar area.
- Dobrymin and Avchyan, 1970-71: Compiled by Adam, 1976 under the title "Geothermal and Geoelectric studies".
- Georgsson I. 1984: Resistivity and temperature distribution of the Reykjanes peninsula, SW Iceland. Society of exploration Geophysicists 54th annual International Meeting.
- Koefoed O. 1979: Resistivity Sounding Measurements. Elsevier Scientific Publishing co. NY.
- Mwangi, M. 1982: Two-dimensional interpretation of Schlumberger sounding and Head on data. UNU report 1982.
- Volarovich M.P. & Parkhomenko E.I: Compiled by Adam A. under the title Geothermal and Geoelectric studies.
- Zhong, B. Zhou, X. Eyjólfsson, B.: Resistivity modelling with finite element method.

Table 1: Resistivity layers and corresponding geohydrological formations in the Reykjanes peninsula.

Geohydrological formation	Resistivity (Ωm)	thickness (m)
Volcanic scoria and/or soil	Variable	2
"Dry" lava	5000 - 25000	approx. elevation of site
Fresh water lens	300 - 3000	30 - 70
Rock penetrated by cold sea water	5 - 15	
Rock penetrated by geothermal brine	2 - 6	

Table 2. One dimensional models of measurements in Krisuvík high temperature area.

<u>Center</u>	<u>Layer</u>	<u>Resistivity</u>	<u>Thickness</u>	<u>Depth</u>	<u>Deviation</u>
TD98	1	105Ωm	2.9m	2.9m	5.2%
	2	319Ωm	76m	78.9m	
	3	6.6Ωm	172m	251.8m	
	4	22.6Ωm			
<hr/>					
TD99	1	62.2Ωm	8m	8m	7.21%
	2	2.7Ωm	144.2m	152.2m	
	3	7.7Ωm	93.2m	245.4m	
	4	37.3Ωm	256.3m	502.7m	
	4	2.5Ωm			
<hr/>					
TD100	1	338.2Ωm	3.5m	3.5m	4.18%
	2	85.9Ωm	54.4m	57.9m	
	3	115.6Ωm	43.5m	101.4m	
	4	2.4Ωm	34m	135.4m	
	5	10Ωm			
<hr/>					
TD101	1	3296Ωm	11.7m	11.7m	22.8%
	2	58Ωm	48.4m	60.1m	
	3	10.5Ωm	35m	95.1m	
	4	114.9Ωm	52.2m	147.1m	
	5	2.41Ωm			
<hr/>					
TD102	1	71.9Ωm	3.8m	3.8m	11.2%
	2	42.6Ωm	43.8m	47.6m	
	3	6.6Ωm	1324m	1371.6m	
	4	8.9Ωm			
<hr/>					
TD103	1	169.5Ωm	23.4m	23.4m	13.2%
	2	25.2Ωm	86.2m	109.6m	
	3	203.9Ωm	156.3m	265.9m	
	4	4.5Ωm			

Table 3. One dimensional models of measurements in Menengai prospect area.

<u>Center</u>	<u>Layer</u>	<u>Resistivity</u>	<u>Thickness</u>	<u>Depth</u>	<u>Deviation</u>
TD 1	1	42Ωm	1.70m	1.7m	16.8%
	2	209Ωm	111.89m	113m	
	3	23Ωm			
TD 9	1	36.8Ωm	0.51m	0.51m	9.5%
	2	149.5Ωm	201.7m	202.2m	
	3	16.41Ωm			
TD 15	1	41.2Ωm	1.5m	1.5m	13.45%
	2	158.7Ωm	231.9m	233.4m	
	3	17.6Ωm			
TD 7	1	259.2Ωm	15.7m	15.7m	13.54%
	2	1252Ωm	14.2m	29.9m	
	3	181.8Ωm	204.3m	204.3m	
	4	10.66Ωm			
TD 17	1	56.8Ωm	3.7m	3.7m	5.78%
	2	174Ωm	83.0m	86.7m	
	3	69.3Ωm			
TD16	1	65.1Ωm	8.7m	8.7m	5.56%
	2	137.4Ωm	207.8m	111.9m	
	3	25.4Ωm			

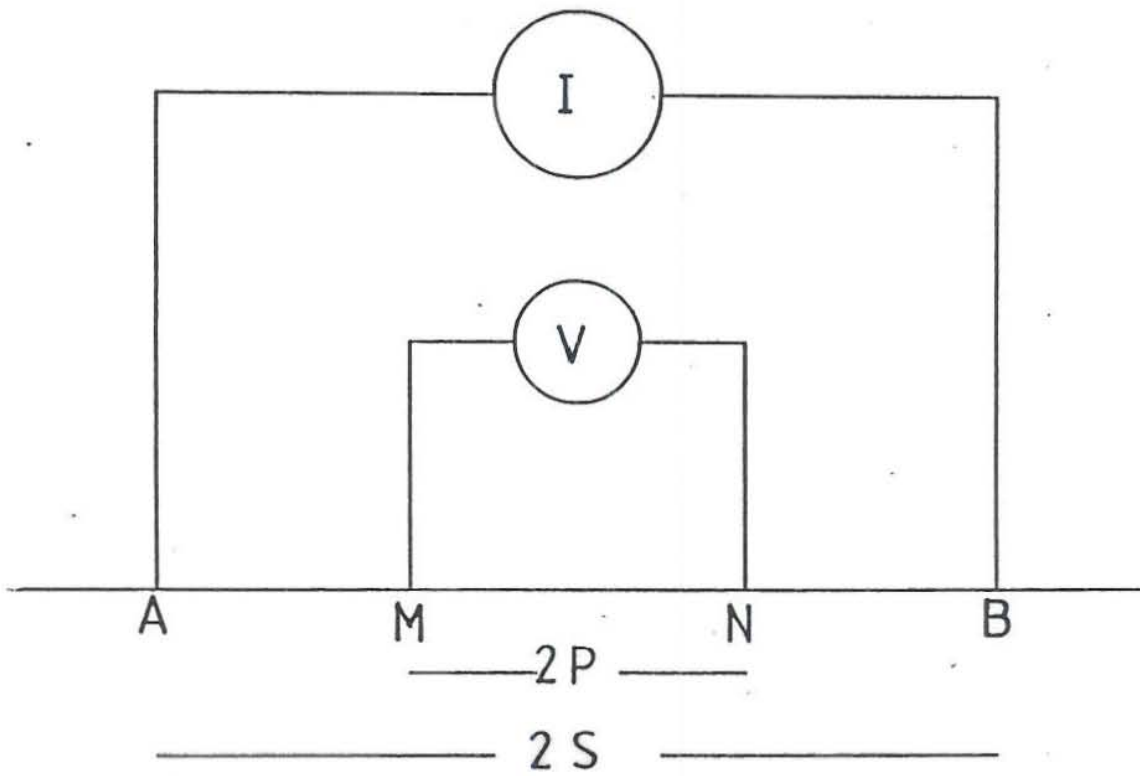
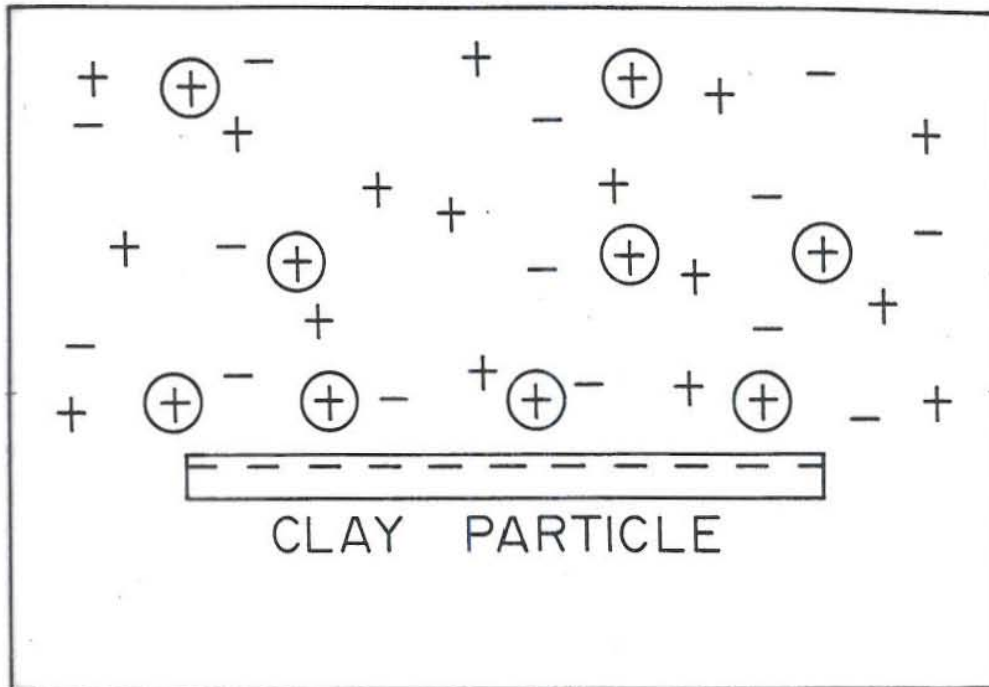
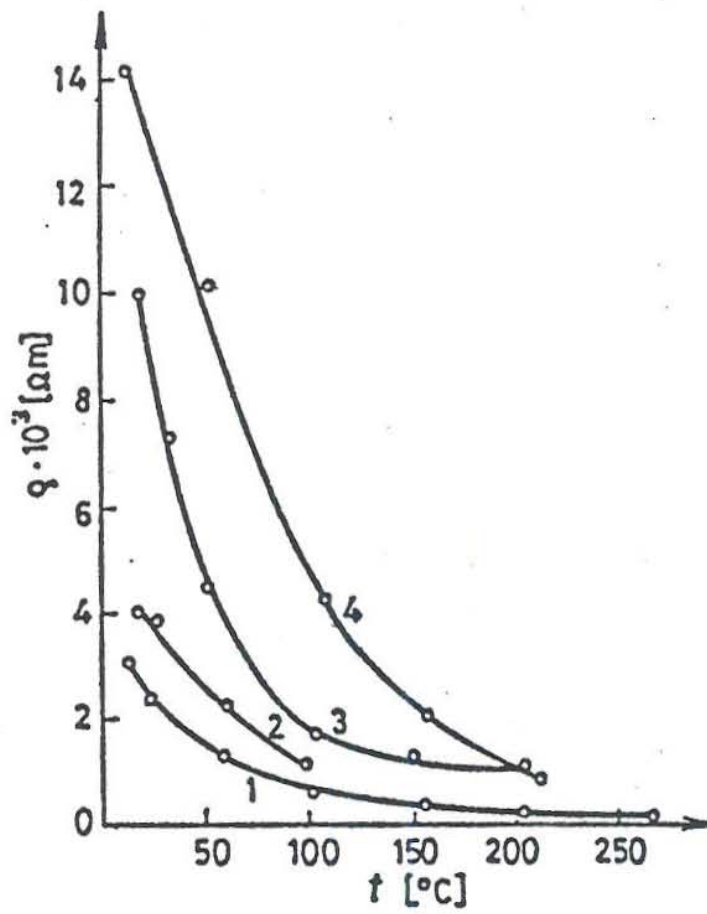


Figure 1. The Schlumberger array configuration.



- ⊕ ADSORBED AND EXCHANGE CATIONS
- + NORMAL CATIONS
- NORMAL ANIONS

Figure 2. Schematic representation of ions adsorbed in clay.



1 - gabbro; 2, 3 - granites; 4 - syenite

Figure 3. Dependence of electrical resistivity on temperature. (Adam A., 1976).

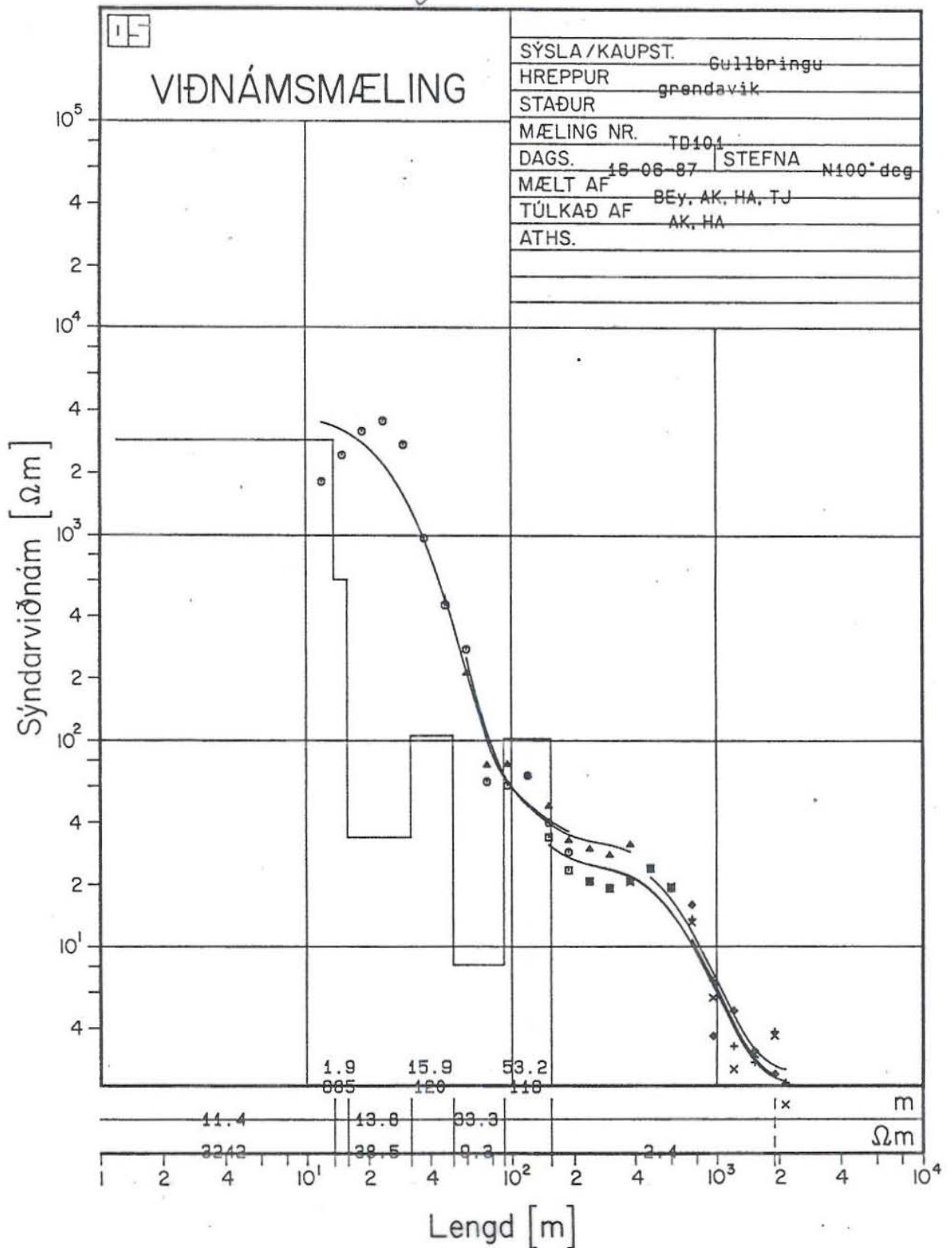


Figure 4. Shifts encountered during data acquisition of measurement TD101 in Krísuvík.

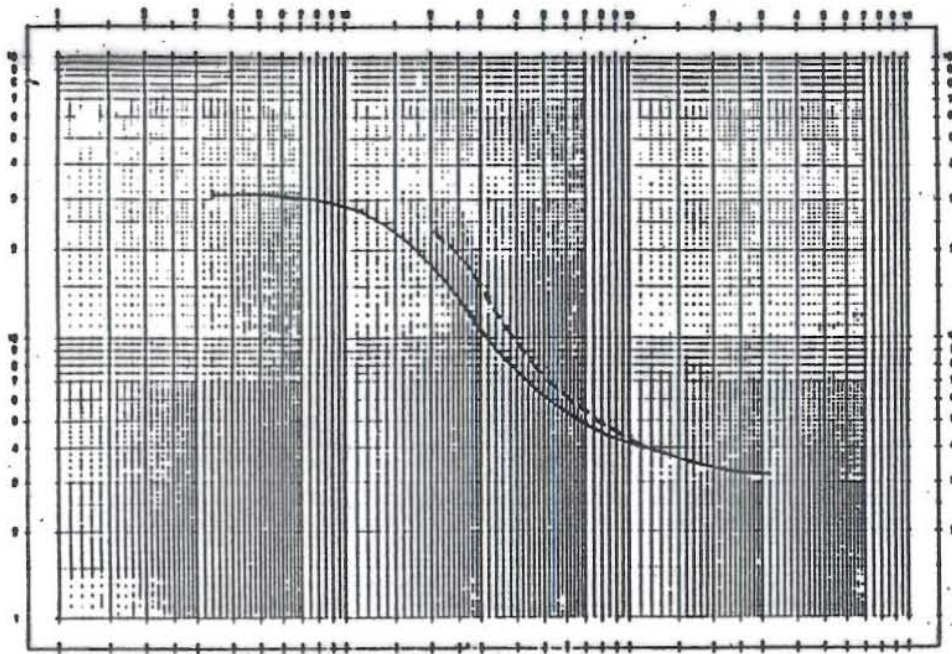


Figure 5a. Converging shifts in apparent resistivity.

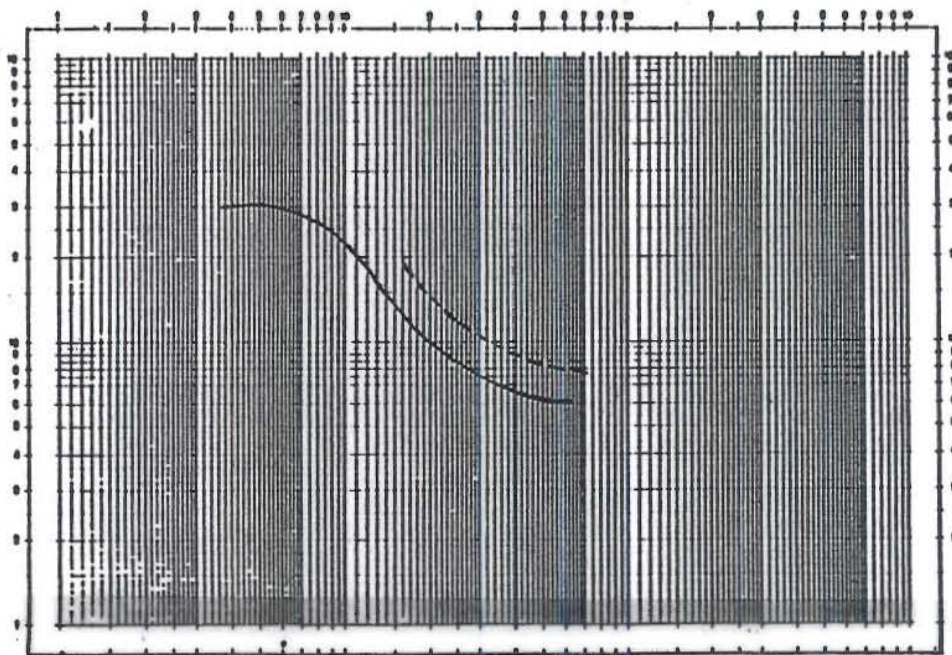


Figure 5b. Nonconverging shifts in apparent resistivity.

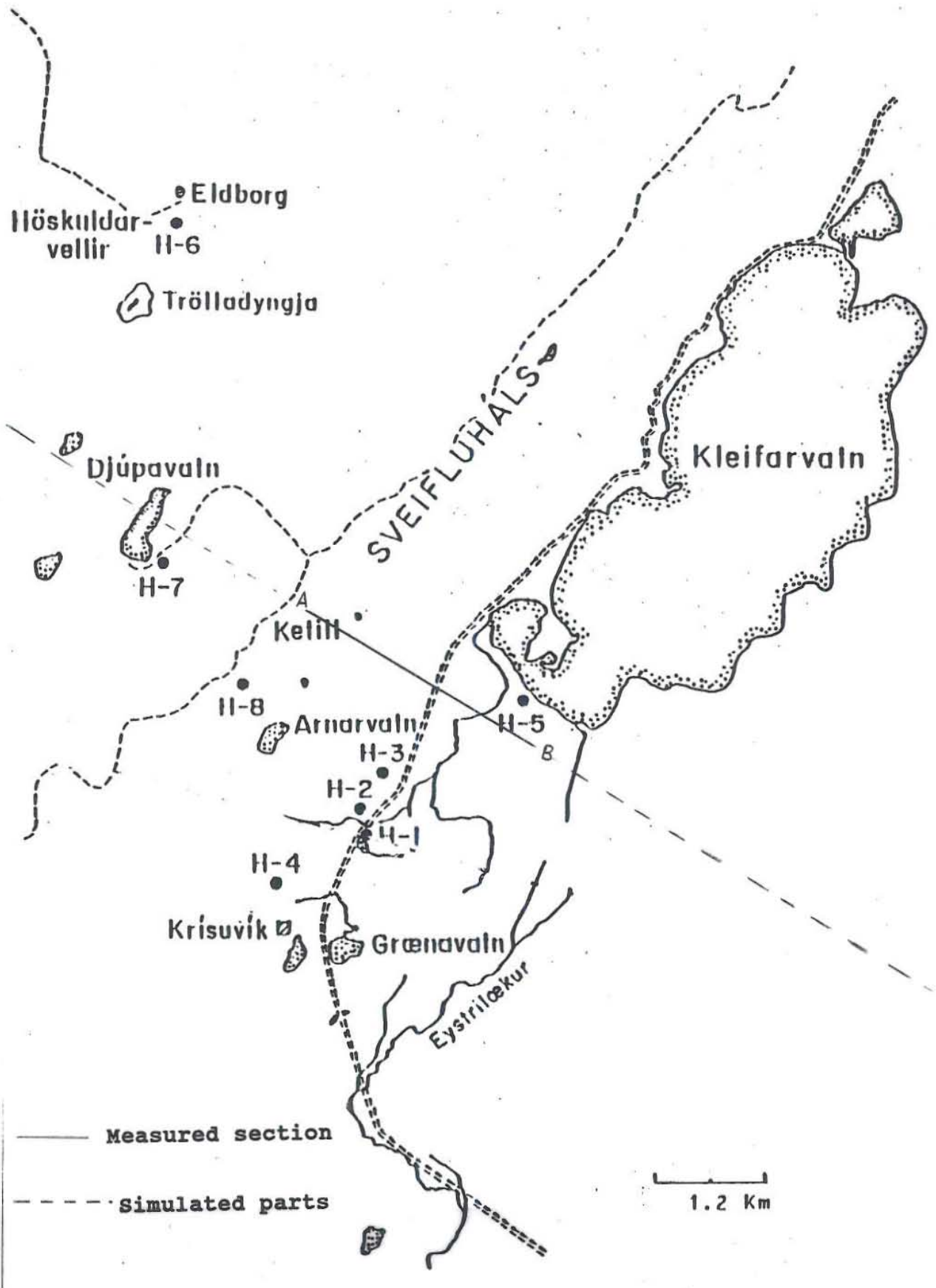


Figure 6. Location of sounding line of measurement at Krísuvík.

KRÍSUVÍK
HIGH-TEMPERATURE AREA
Electrical resistivity
at 600m depth

-  < 10 $\Omega\cdot\text{m}$
-  10-30 $\Omega\cdot\text{m}$
-  30-50 $\Omega\cdot\text{m}$
-  > 50 $\Omega\cdot\text{m}$
-  Resistivity uncertain
due to few measurements

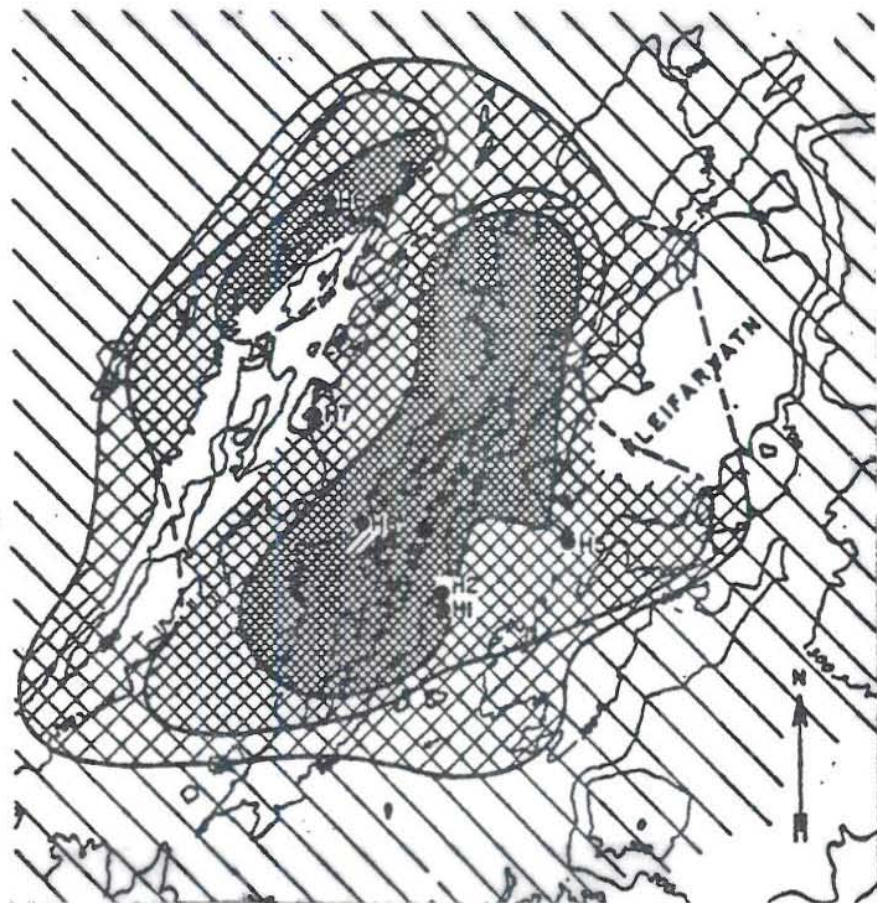
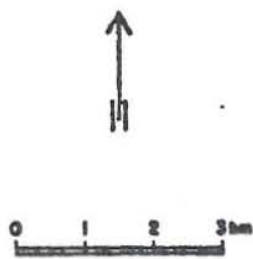


Figure 7. Apparent resistivity at 600m depth in Krísuvík.



Figure 8. Location of measurements in Menengai prospect area.

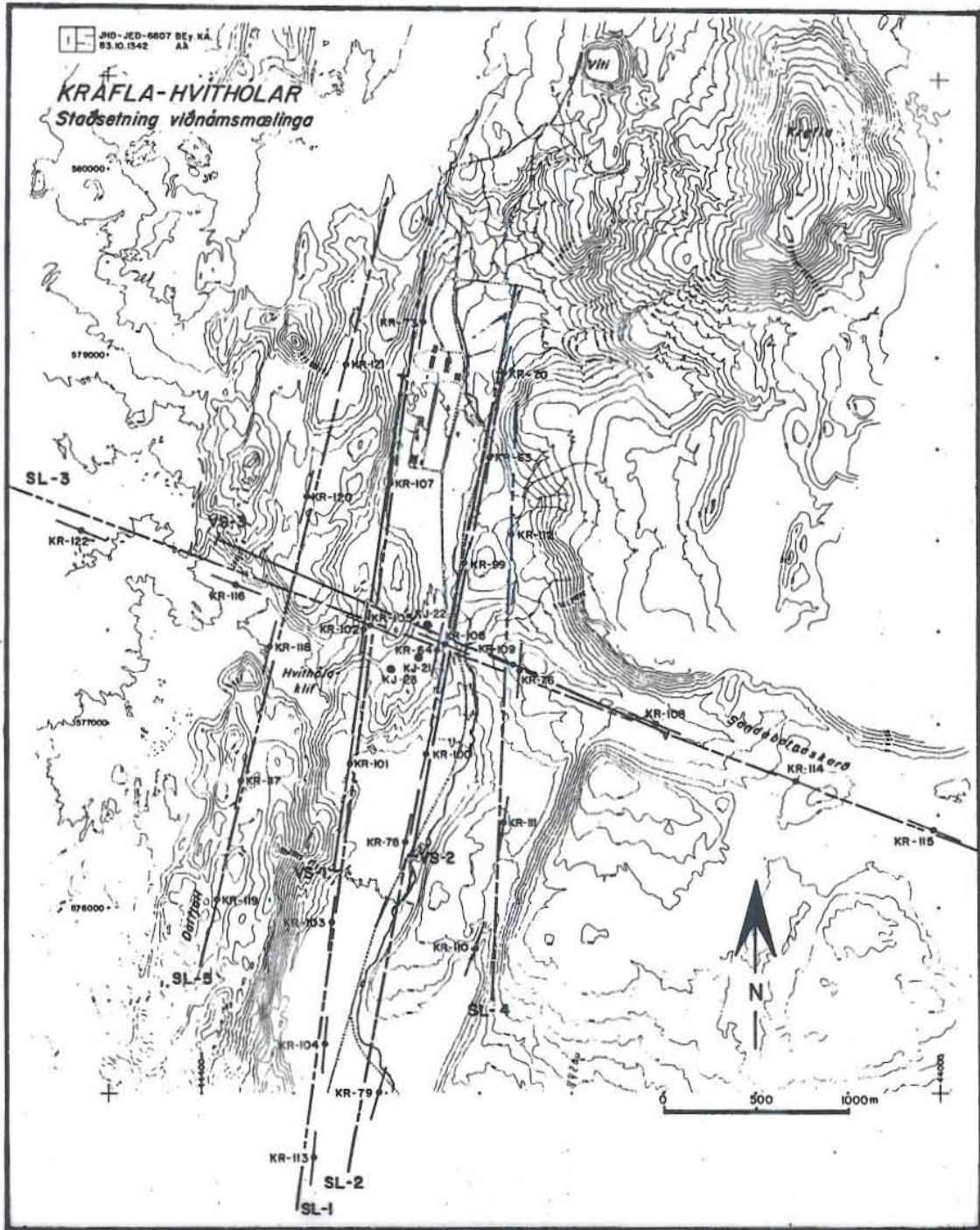


Figure 9. Resistivity measurement lines at Krafla - Hvithólar. (Björnsson, A., 1984).

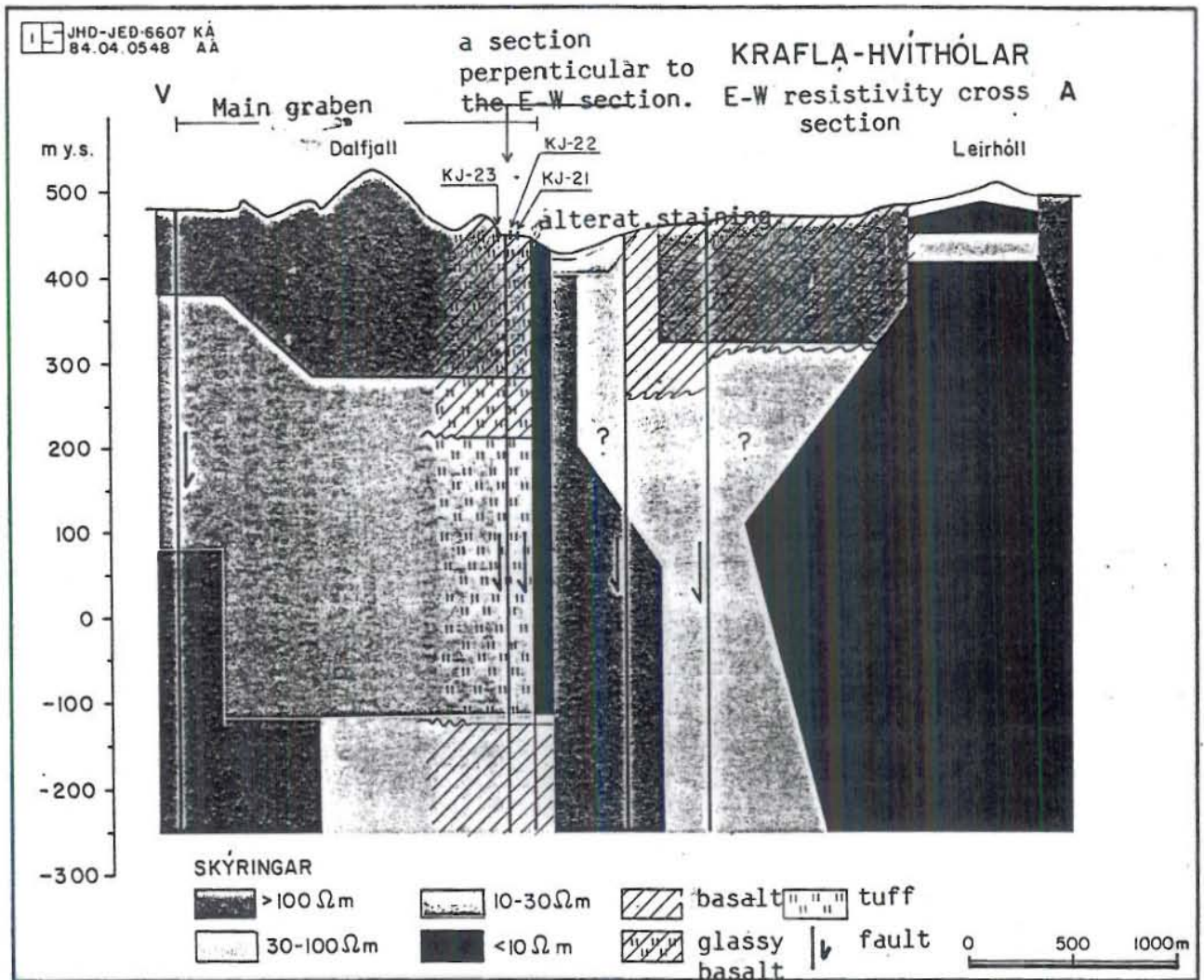


Figure 10a. Krafla - Hvitholar; cross section of E - W resistivity distribution.
(Björnsson, A., . 1984)

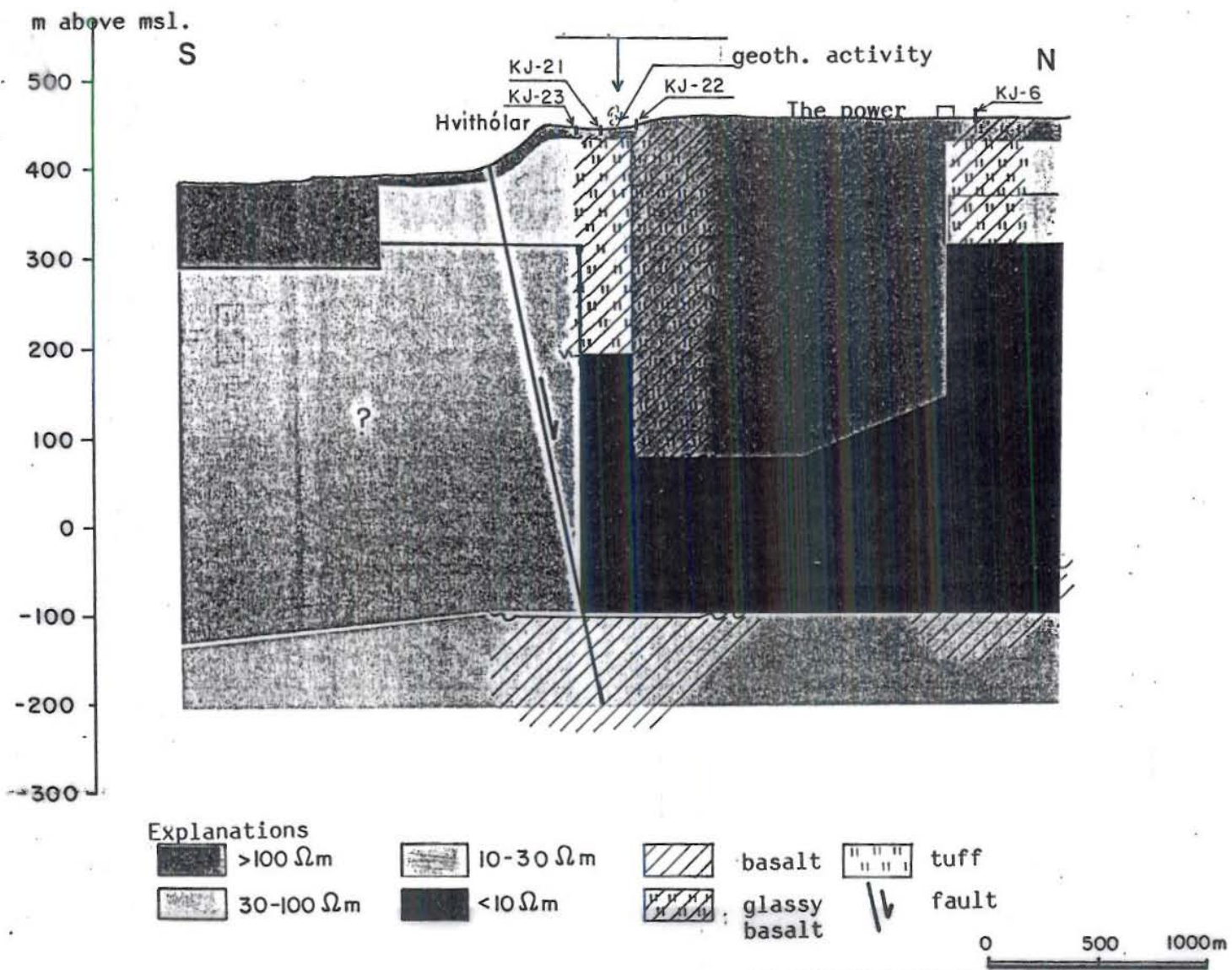
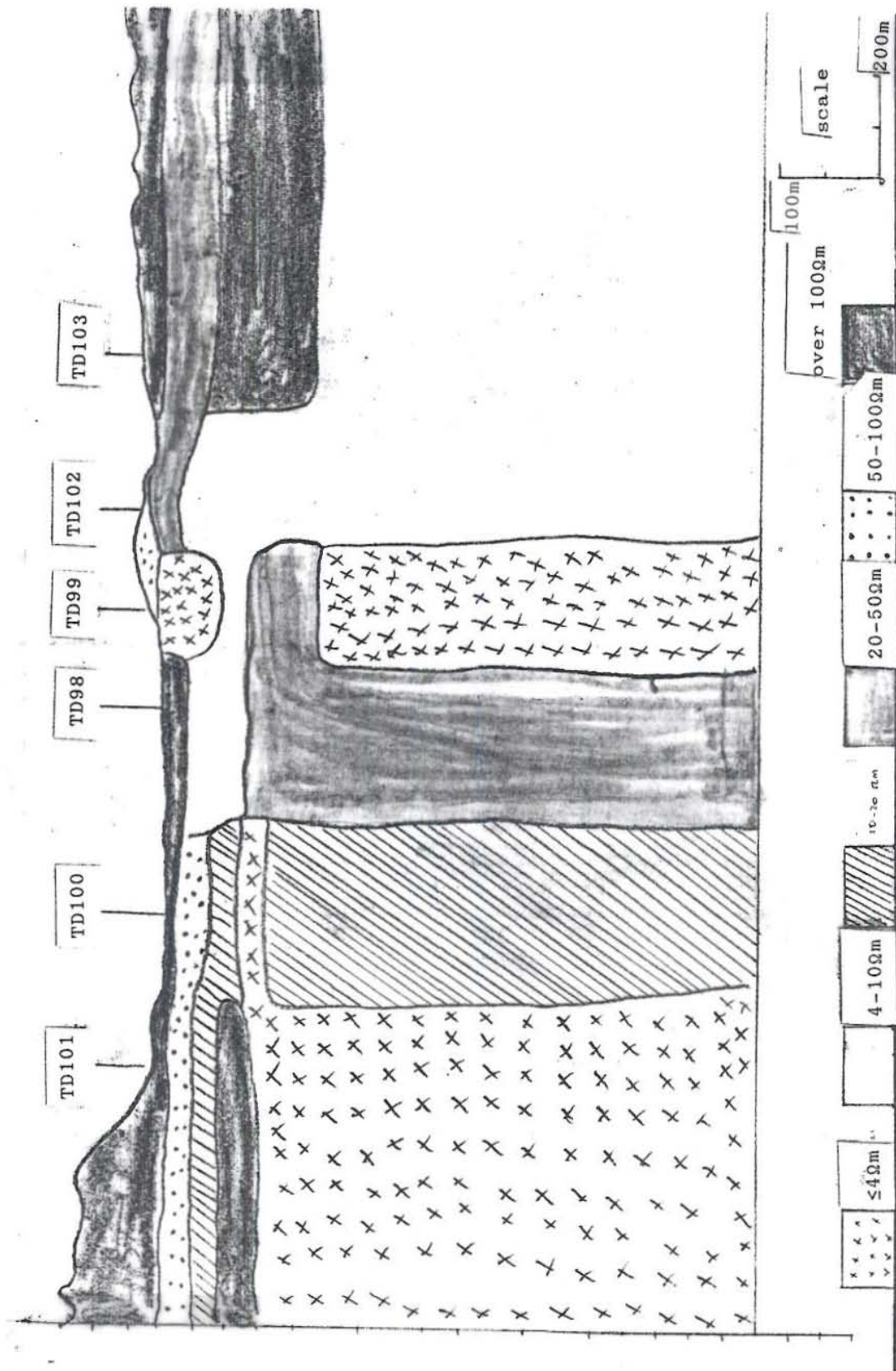
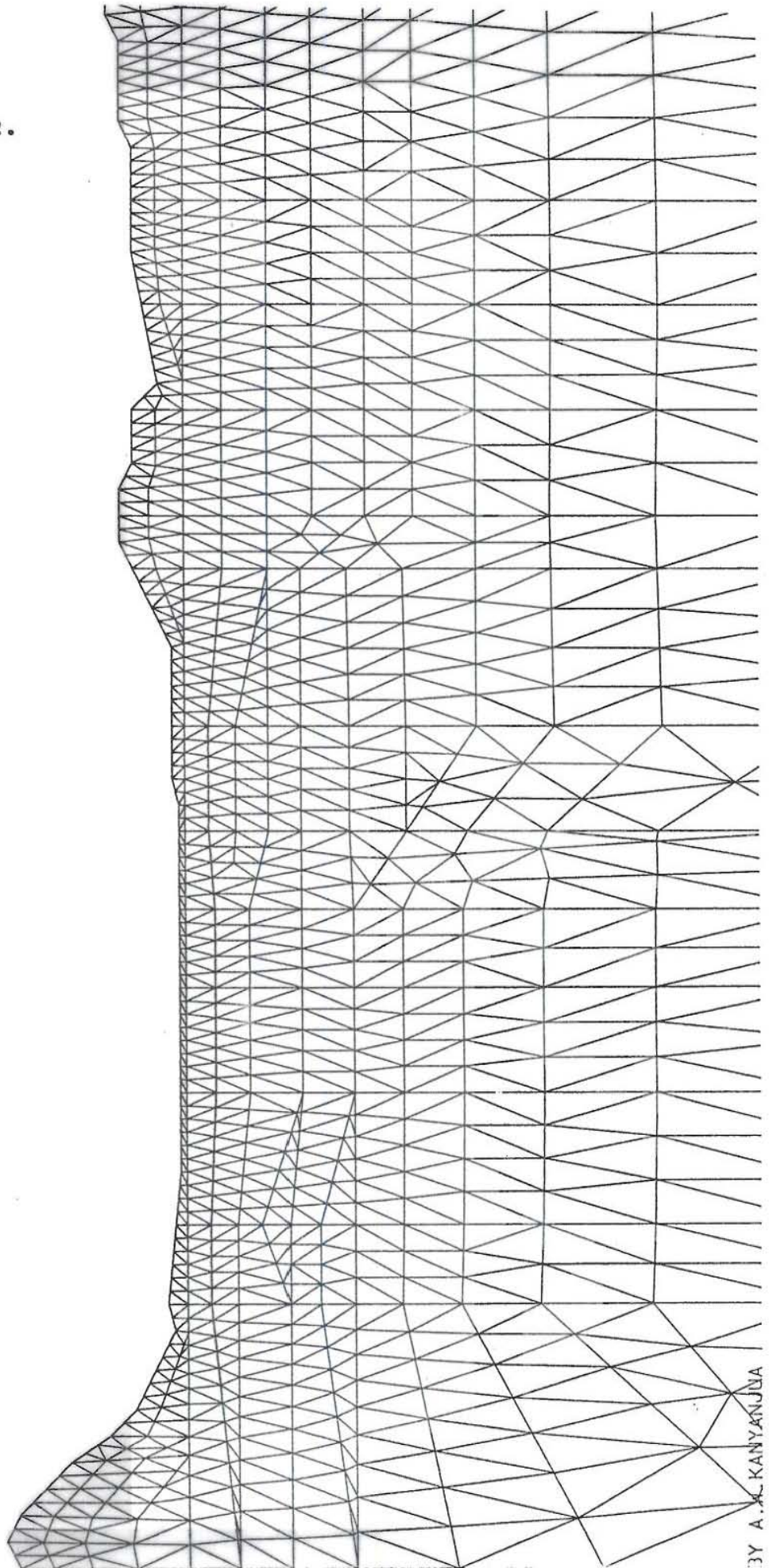


Figure 10b. Krafla - Hvithólar; cross section of resistivity distribution perpendicular to the E - W direction. (Björnsson, A., 1984).

APPENDIX 1.



APPENDIX 2.



BY A. L. KANYANJUA



